Journal of Solid State Chemistry **155,** 9–14 (2000)
doi:10.1006/jssc.2000.8880, available online at http://www.idealibrary.com on IDEAL®

New Ternary Lanthanide Transition-Metal Tellurides: Dy_6MTe_2, M = Fe, Co, Ni

Naima Bestaoui, P. Subramanya Herle, and John D. Corbett[1]

Department of Chemistry, Iowa State University, Ames, Iowa 50011

Received May 16, 2000; in revised form July 17, 2000; accepted July 17, 2000

DEDICATED TO PROFESSOR J. M. HONIG

The isotypic title compounds together with R_6CoTe_2 for R = Y, La have been synthesized in Ta containers at high temperature and their lattice parameters refined from Guinier X-ray powder diffraction data. The structure of this family has been detailed in space group $P\bar{6}2m$ ($Z = 1$) by single-crystal X-ray diffraction data for the case of Dy_6FeTe_2 ($a = 8.236(3)$ Å, $c = 4.0107(2)$ Å, 23°C, $R(F)/R_w = 3.6/3.8\%$). The overall structure is of the Zr_6CoAl_2 type, an ordered derivative of the Fe_2P type. Extended Hückel calculations help to interpret the stabilization of this structure by iron or electron-richer elements. Strong Dy–Fe interactions in more 1D chains are a noteworthy feature.

1. INTRODUCTION

The exploration of new materials is an important step in chemistry. This has led to the discovery of many compounds with diverse properties as well as to a better understanding of structure, bonding, and what is possible in the solid state. Among metal-rich compounds, it has been known for some time that optimal metal–metal bonding is sometimes achieved through formation of clusters or their condensation products when these are stabilized by interstitial heteroatoms. The stability can usually be attributed to strong bonding between the interstitial, often a late transition metal, and a surrounding host metal from an early metal group, a circumstance that is another reminder of some early ideas of Brewer (1). Among the many reduced chalcogenides of the early transition metals that demonstrate these heterometal features are $Ta_9M_2S_6$ (2, 3), $Ta_{11}M_2Se_8$ (4), Ta_8MSe_8 (5), Nb_6MS_2 (6), Hf_5MTe_3 (7), all with some combination of M = Fe, Co, Ni, Zr_6MTe_2 (M = Mn, Fe, Co, Ni, Ru, Pt) (8), Hf_8MTe_6 (9) (M = Mn–Fe), $Nb_9Ni_{2-x}S_{3+x}$ (6), Ta_4MTe_4 (M = Cr, Fe–Ni, Al, Si) (10,11), $Sc_5Ni_2Te_2$ (12), $Y_5M_2Te_2$ (M = Fe–Ni) (13), and Sc_6MTe_2 (14) (M = Mn–Ni). Many of these phases also have a common structural motif, have tricapped trigonal prismatic clusters of the more active metal that share basal faces, and are centered by the late transition metal. A second large area of compounds that exhibit cluster stabilization by late transition metal interstitials M is transition group 3 and 4 metal (T) cluster halides (X) of the $T_6(M)X_{12+n}$ types. In these cases, M always centers individual octahedra of the earlier metal T. Condensation of these into diverse oligomers, chains, or sheet products is also found (15).

In general, there has been a dearth of reports of metal-rich chalcogenides of the lanthanide elements. In this article we report on the syntheses, structure, and bonding of the first such compounds, namely for the ternary Dy_6MTe_2 (M = Fe, Co, Ni, and Pt) together with La and Y examples for M = Co. These are analogues of reduced ternary scandium chalcogenides that exhibit heterometal-centered tricapped trigonal prismatic clusters as basic structural building blocks (12) and which include the isostructural phases Sc_6MTe_2, M = Mn–Ni (14). The bonding and stability of the present structures will also be considered in terms of the results of extended Hückel band calculations.

2. EXPERIMENTAL SECTION

Syntheses

All the materials were handled in controlled atmosphere gloveboxes filled with He or N_2. The Dy utilized was from Ames Laboratory (99.99%), the Fe from Alfa (> 99.5%), and the Te came from Aldrich (99.99%).

These compounds were first observed after reactions of the elements Dy, M, and Te near the atom proportions 6:1:2 in sealed niobium tubes in which these had first been prereacted at 700°C for 24 h to immobilize the Te. The resulting material was pelletized and arc-melted, and the buttons were then sealed inside tantalum tubes and annealed. Different conditions for annealing were tested, and the best was found to be 1200°C for three days. However,

[1]To whom correspondence should be addressed.

0022-4596/00 $35.00

these conditions were not completely satisfactory as the resulting products contained only around 85% Dy_6MTe_2 according to the powder patterns, the rest being DyTe. The evident loss of 3d M components into Nb or (less) Ta containers has been noted before in other systems (16,17). The synthesis of Dy_6NiTe_2 was also explored starting with Dy_4Te_{11}, Ni_2Te_3, and Dy in the proper proportions. These components, pressed into a pellet and sealed directly into a more refractory tantalum tube, were heated (in a silica jacket) at 1400°C for two hours and then at 800°C for two weeks. The prior arc-melting step seems important as this route gave yields of only $\sim$70%.

The optimized reactions subsequently developed utilized stoichiometric proportions of Dy, $DyTe_2$, and M (M = Fe, Co, or Ni) for the composition Dy_6MTe_2. The weighed components were mixed, pressed into a pellet, and this was then arc-melted twice, 30 s on each side, in a melter accessed from within another glovebox. The weight losses during this step never exceeded 1%. The arc-melted specimen was then wrapped in Mo foil (to minimize loss of the transition metal into the container) and welded into 9.5-mm diameter Ta tubing that was in turn sealed into a silica jacket under vacuum, as customary (12). The assembly was then heated for one week at 1100°C followed by two weeks at 800°C. The title compounds Dy_6MTe_2 were obtained in this way in high yields (95%) from these compositions according to their Guinier powder patterns, assuring the basic correctness of the X-ray composition. A second phase in the patterns was always a trace of DyTe (NaCl type), for which a small continuing loss of M into the Ta was thought responsible. No evidence of any other phase was observed in the powder patterns. Inclusion of Mn, Pt, or Cu as the potential transition element did not give this structure.

Some attempts to synthesize the same phases for Y or La instead of Dy led to the formation of the 6:1:2 phase just for Co but with a lower yield, especially in the case of La, where LaTe binary appears to be relatively more stable.

Powder Diffraction

The diffraction patterns of the powdered products were obtained with the aid of an Enraf–Nonius Guinier camera and monochromatic Cu$K\alpha_1$ radiation. The samples were each crushed into powder, mixed with a silicon standard (NIST), and placed on a frame between two strips of cellophane tape for mounting in the camera. The hexagonal lattice parameters listed in Table 1 were obtained by least-square refinements of the indexed and measured θ values. The latter were determined with the aid of a nonlinear fit to the positions of the standard Si lines. The lattice parameters are quite similar over the series. Both increase on passing from Dy to La (with Co) or Co to Fe (Dy), but a decreases and c increases on going from Dy to Y (Co) or from Co to Ni (Dy).

TABLE 1
Lattice Parameters (Å) and Cell Volumes (Å^3) of R_6MTe_2 Compounds ($P\bar{6}2m$)[a]

R	M	a	c	V
Dy	Fe	8.236(1)	4.0107(2)	235.6(2)
Dy	Co	8.176(3)	3.962(2)	229.4(3)
Dy	Ni	8.114(5)	3.991(1)	227.6(4)
Y	Co	8.116(5)	4.003(1)	231.21(6)
La	Co	8.238(4)	4.023(4)	236.5(5)

[a]Calculated from Guinier powder pattern data with Si as an internal standard, λ = 1.540 562 Å, 23°C.

Single-Crystal Diffraction

Several black crystals of the iron compound were mounted into 0.3-mm capillaries in a glovebox, and these were then sealed and mounted on metal pins. Their quality was checked by Laue photographs, and the best one was selected for data collection, a very thin plate, $0.08 \times 0.03 \times 0.005$ mm. Twenty-five centered reflections obtained on a Rigaku diffractometer (Mo$K\alpha$ radiation) at room temperature were used for provisional lattice parameters and an indication of the crystal system. An entire sphere of data was collected to $2\theta_{max} = 60°$ for the indicated hexagonal cell. Of the 2764 measured reflections, 171 were unique ($R_{int} = 0.096$ for $I_o > 0$). The intensities of three representative reflections measured after collection of every 150 reflections remained essentially constant throughout data collection, indicating crystal and electronic stability. An empirical absorption correction was applied with the aid of three ψ-scans, which resulted in relative transmission factors ranging from 0.17 to 1.00.

The Laue check on data reduction indicated a 6/*mmm* class. At this point, the similarity to Zr_6MTe_2 (8) was recognized, and the structure was solved by direct methods (SHELXS) (18) and refined with the package TEXSAN (19) in the corresponding space group $P\bar{6}2m$ (No. 189). Thermal parameters were first refined isotropically. The original data were then averaged ($R_{ave} = 0.09$, $I > 0$), and the anisotropic displacement parameters refined. The final cycle of full-matrix least-squares refinement on F, with 164 observed reflections and 13 variables, converged with unweighted and weighted agreement factors of $R(F) = 0.036$ and $R_w = 0.038$. The maximum and minimum peaks in the final difference Fourier map corresponded to 3.54 and -2.78 e$^-$/Å^3, respectively. The F_o/F_c listing is available from J.D.C.

Band Calculations

Extended Hückel band calculations for Dy_6FeTe_2 were carried out within the tight binding approximation (20) at

156 k-points spread over the irreducible wedge. The program CAESAR (21) was utilized for this purpose. The parameters employed and their sources are described in a later section.

3. RESULTS AND DISCUSSION

Structure of R_6MTe_2

This family of isostructural compounds was obtained with Co for the rare-earth elements La and Y and with several late transition metals M = Fe, Co, Ni in the instance of Dy (Table 1). Tables 2 and 3 list the data collection parameters and the positional and thermal parameters for Dy_6FeTe_2, respectively. An overall view of a section of the structure nearly along [001] is presented in Fig. 1 while Fig. 2 shows the repeat unit and distances in the chain along $\vec{c}$. The nearest neighbor distances in Dy_6FeTe_2 are given in Table 4. The structure is constructed from confacial trigonal prisms of Dy1 (inner) centered by the transition metal (Fe), with Dy1–Dy1 distances of 3.402(4) Å within the shared triangular faces and 4.011 Å along the c axis. Each rectangular face of the trigonal prism is capped by a Dy2 atom (outer) with Dy1–Dy2 distances of 3.496(2) Å. This collection of atoms yields the very familiar tetrakaidecahedra (tricapped trigonal prisms) that are each centered by the transition metal M and interconnected through shared basal Dy1 faces along the c axis into infinite chains. Figure 1 also shows how columns of these condensed tetrakaidecahedra are interconnected normal to [001] into a hexagonal pattern via 3.598(3) Å Dy1–Dy2 interchain bonds, 0.10 and 0.20 Å longer than those within the augmented trigonal prisms. (These numbers compare with 3.56 Å in the h.c.p. metal and 3.20 Å for the Pauling single bond value (22).) The interchain separation is relatively larger than in Sc_6FeTe_2 (14). The tellurium atoms are similarly surrounded by nine Dy that generate the inverse tetradekaidecahedra around the chalcogens, but of very different proportions, with three capping Dy1 about each Te in the same plane and Dy2 in the trigonal prism at 3.199(4) and 3.210(2) Å, respectively. These very similar values suggest that both are determined mainly by closed shell contacts for Dy^{+3} and Te^{-2} oxidation states; the sum of Shannon crystal radii for Dy^{+3} (CN8) and Te^{-2} is 3.24 Å (23). In contrast, the transition metals (Fe) center differently

TABLE 2
Crystal and Data Collection Parameters for Dy_6FeTe_2

Formula weight	1286.05
Crystal color, habit, dimensions (mm)	Black, plate-like, $\sim 0.080 \times 0.032 \times 0.005$
Crystal system, space group, Z^a	hexagonal, $P\bar{6}2m$ (No. 189), 1
d_{calc} (g/cm^3)	9.127
μ (Mo$K\alpha$, cm^{-1})	553.05
Data collection	
Diffractometer	Rigaku AFC6R
Radiation, λ (Å)	Mo$K\alpha$, 0.71069
Temperature	23°C
Scan type	ω–2θ
Octants measured; $2\theta_{max}$	$\pm h$, $\pm k$, $\pm l$; 60°
Refinement	
Measured reflections	2764
Unique reflections, R_{int}, % ($I > 0$)	171, 9.6
Observed reflections ($I > 3\sigma I$)	164
No. of variables	13
Absorption correction	Empirical, 3 ψ scans
Rel. transm. coeff. range	0.17–1.00
Largest residual peak (e$^-$/Å^3)	3.54
R, R_w[b]	0.036, 0.038
Goodness of fit	3.47

[a] Lattice dimensions in Table 1.
[b] $R = \sum||F_o| - |F_c||/\sum|F_o|$; $R_w = [\sum w(|F_o| - |F_c|)^2/\sum w(F_o)^2]^{1/2}$; $w = \sigma_F^{-2}$.

TABLE 3
Positional and Thermal Parameters Data for Dy_6FeTe_2

Atom	Wykoff position	x	y	z	B_{eq}[a]
Dy1	3f	0.2385(2)	0	0	0.73(8)
Dy2	3g	0.6011(3)	0	$\frac{1}{2}$	0.76(8)
Fe	1b	0	0	$\frac{1}{2}$	0.64(7)
Te	2c	$\frac{1}{3}$	$\frac{2}{3}$	0	1.5(3)
Atom	U_{11}[b]	U_{22}	U_{33}		
Dy1	0.0079(9)	0.007(1)	0.0124(6)		
Dy2	0.0116(9)	0.008(1)	0.0080(6)		
Te	0.008(1)	U_{11}	0.009(1)		
Fe	0.0025(5)	$U11$	0.008(4)		

[a] $B_{eq} = (8\pi^2/3)\sum_i\sum_j U_{ij}\vec{a}_i\vec{a}_j$.
[b] $T = \exp[-2\pi^2(U_{11}h^2a^{*2} + U_{22}k^2b^{*2} + U_{33}\ell^2c^{*2} + 2U_{12}hka^*b^*)]$; $U_{13} = U_{23} = 0$, $U_{12} = U_{22}/2$.

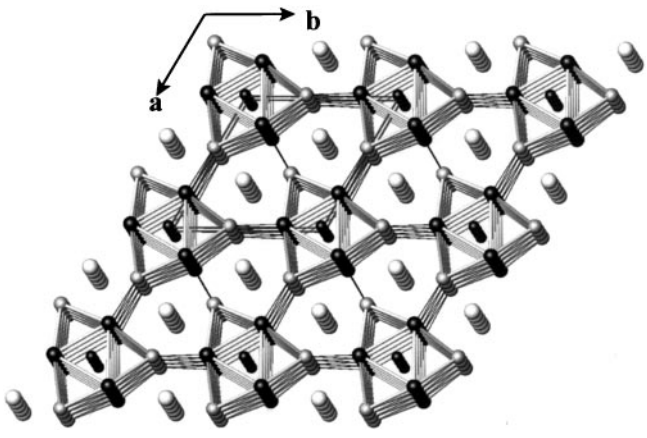

FIG. 1. Off-[001] section of the hexagonal Dy_6FeTe_2 structure with the cell marked. Dy1, ●; Dy2, ○; Fe within Dy chains, ●; Te in open channels, ○. Dy–Dy bonds are outlined up through 3.60 Å.

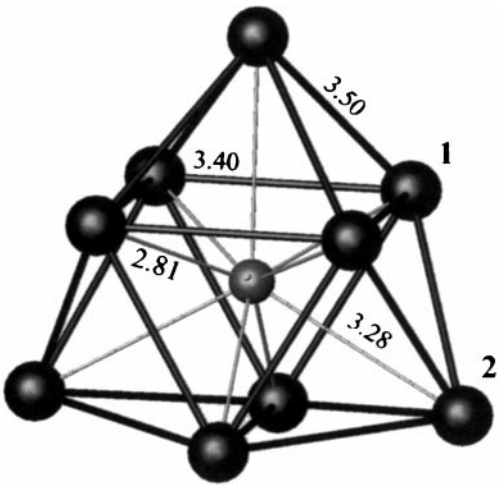

FIG. 2. Detail of tricapped trigonal prism of Dy about centered iron atom (smaller) with relevant distances (Å).

proportioned tricapped trigonal prisms of Dy, 2.800(3) Å to inner Dy1 with the face-capping Dy2 that lie in the same plane as Fe nearly 0.5 Å further away. The latter presumably reflect intrinsic bonding effects. The average Fe–Dy distance, 2.96 Å (×9), is close to that found in $DyFe_2$ ($MgCu_2$ type), 3.04 Å (×12) (24).

The parent structure of these compounds is the Fe_2P type $[Fe_6(P)P_2]$ (25) in which the two independent phosphorus positions correspond to *M* and 2Te. A closer relationship exists with not only Sc_6FeTe_2 (14) but also the equivalent ternaries Zr_6MAl_2 (M = Fe, Co, Ni) (the parent structure type is the Co member (26)) and Zr_6FeSn_2 (16). Electron-richer ternary tellurides that also adopt this structure type are Zr_6MTe_2 (M = Mn, Fe, Co, Ni, Ru, or Pt) (8). The versatility and flexibility are remarkable.

TABLE 4
Important Interatomic Distances (Å) and Overlap Populations in Dy_6FeTe_2

Atom	Atom	Distance	Overlap population[a]
Dy1	Dy1 (×2)	3.402(4)	0.307
Dy1	Dy2 (×4)	3.496(2)	0.230
Dy1	Dy2 (×2)[b]	3.598(3)	0.127
Dy1	Fe (×2)	2.807(1)	0.219
Dy2	Fe	3.285(2)	0.098
Dy1	Te (×2)	3.208(1)	0.229
Dy2	Te (×4)	3.2199(7)	0.240
Dy1	Dy1	4.0107(2)[c]	0.144
Dy2	Dy2	4.0107(2)[c]	0.064
Fe	Fe	4.0107(2)	−0.004[c]

[a]Per atom pair.
[b] Interchain.
[c] *c* axis repeat.

Band Structure Results

The selection of parameters for band calculations on unconventional compounds such as Dy_6FeTe_2 requires some thought regarding the H_{ii} values, particularly those for iron. Program default values for metals are usually those suitable for more or less conventional neutral or positive oxidation states. On the other hand, Fe bonded to a more electropositive element, as an interstitial in effect, appears to be reduced below the neutral state (judging from Mulliken atom populations). This serves to raise the H_{ii} values correspondingly and, often, to increase the resultant mixing with valence orbitals of a more active host metal. To some extent, this may be corrected for by iterations of the energies to charge consistency. Some earlier examples of this approach are for Zr_6FeI_{14} (27), Zr_6FeTe_2 (8), Gd_3MnI_3 (28), $Sc_5Ni_2Te_2$ (12), $Y_5Fe_2Te_2$ (13), and Sc_6FeTe_2 (14). Furthermore, XPS core shifts indicate a similar sort of effect in Ca_5FePb_3 vs other iron phases (29). For our purposes, we started the interation with values for Dy from those calculated for Gd in Gd_3MnI_3 and for Fe from the data in Y_5FeTe_2. The Te value came from studies of the above scandium tellurides while the charge vs energy and Slater orbital parameters were taken from Alvarez (30). All of the data employed are summarized in Table 5.

The total densities-of-states (DOS) calculated for Dy_6FeTe_2 is presented in Fig. 3, with the individual contributions of Dy (dashed) and Fe (dotted) projected out. COOP (overlap-weighted pair population) data as a function of energy are shown in Fig. 4 for the Dy–Dy (solid) and Dy–Fe (dotted) interactions. Tellurium 5p is the principal component of a band between about −16.5 and −14.0 eV (not shown), with small contributions from Dy representing some covalency in the Dy–Te bonding. The contribution of Fe orbitals is primarily seen in the larger d band around −8.3 eV, while only Dy makes major contributions to the conduction band above about E_F, −7.17 eV. The Fermi level passes through the bottom of a band with strongly bonding Dy–Dy and moderately antibonding Fe–Dy states

TABLE 5
Parameters for Extended Hückel Calculations on Dy_6FeTe_2

Orbital	H_{ii} (eV)	ς_1	ς_2	C_1	C_2
Dy 6s	−6.73	1.47			
6p	−4.18	1.47			
5d	−6.33	2.778	1.2415	0.7123	0.4640
Te 5s	−21.2	2.51			
5p	−12.0	2.16			
Fe 4s	−5.97	1.9			
4p	−2.81	1.9			
3d	−7.60	5.35	2.00	0.5505	0.6260

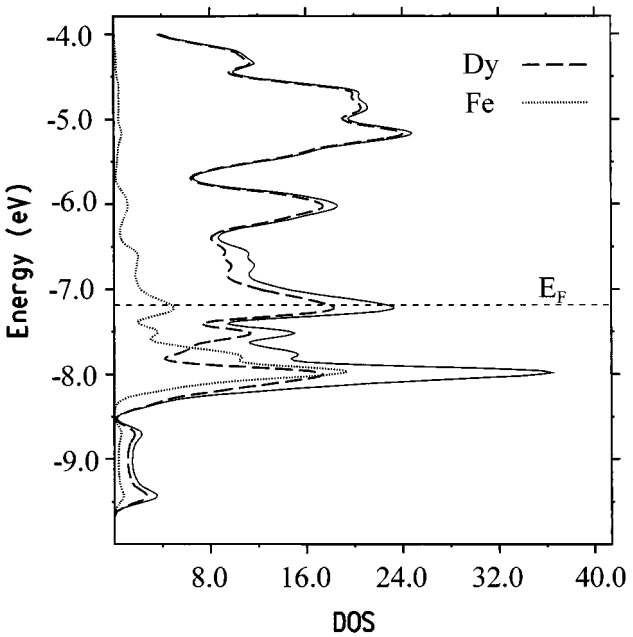

FIG. 3. DOS curve (solid line) for Dy_6FeTe_2 with the Dy (dashed) and Fe (dotted) contributions projected out. The Te 5p contributions are off-scale, between -14.0 and -16.5 eV.

(Fig. 4). The overall width of the d band is notably larger than that for Sc_6FeTe_2. A metallic character of the compound is implied, as would be intuitively expected from the structure as well. The COOP data for Dy–Fe interactions

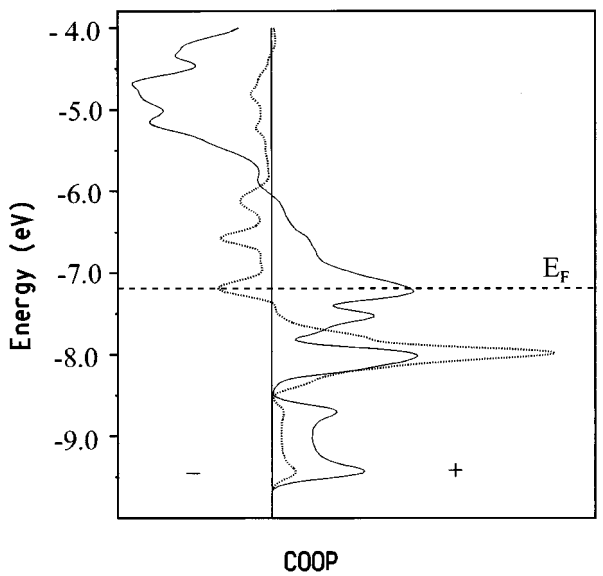

FIG. 4. The COOP properties of Dy_6FeTe_2 for all Dy–Dy (solid line) and Dy–Fe (dotted) interactions as a function of energy. The populations to the right are bonding (positive).

again emphasize an appreciable Dy–Fe covalency. The clean separation between Fe and Te components is of course a reflection of the structure, where these are well separated by Dy atoms.

The bond overlap population (OP) data integrated up to E_F for each of the pairwise interactions were given in Table 4 with the corresponding distances. The Dy–Fe bonding occurs at relatively lower energies and with a large Dy1–Fe overlap population suggesting strong polar covalent bonds. Only the Dy–Dy interactions in the tricapped trigonal prisms are comparable. (Of course, one cannot quantitatively compare OPs for different atom pairs because of the atom-dependent overlap integrals included in each type.) A sense of charge transfer from Dy to Fe as well as to Te seems clear. Charges per atom according to the Mulliken definition (which divides bond populations equally) and within the extended Hückel approximation are Dy, $+0.18$; Fe, -0.35; and Te, -0.38. (Actually, the dysprosium charge is distributed about 2:1 on Dy2, presumably because of its greater number of tellurium neighbors.) The OP difference for Dy–Dy bonds between interchain (Dy1–Dy2, 3.60 Å) and average intrachain (prismatic) separations of 3.40–3.50 Å is nearly 47%; even the OP for the 4.01 Å Dy1–Dy1 c axis repeat is larger than the former. Thus the strongest metal–metal glue is within the 1D Fe-centered chains, whereas the lattice beyond these is held together by more typical polar bonding about Te. The tricapped trigonal prisms of Dy about Te are much too large to have meaningful Dy–Dy bonding (4.36 Å for Dy2–Dy2). To some extent the result can be viewed as a Dy sublattice that has been propped open by the Fe and Te atoms (matrix effects).

The corresponding results for Dy_6NiTe_2 were not pursued in part because of the lack of distance detail, but also because we can already anticipate the major differences. The 3d levels on Ni, and therefore the mixing with Dy, will be notably lower and more corelike. These characteristics have already been seen not only for Sc_6MTe_2, M = Fe vs Ni (14), but also in the double-metal-layered La_2Ni_2I (31).

Finally, comparison of Sc vs Dy interactions with iron in the isoelectronic 6–1–2 phases gives some interesting contrasts in their orbital properties. The d band breadth and the implied strength of the interactions of Sc with Fe is distinctly greater for Dy–Fe. The Mulliken atom charges are in parallel (Sc, $+0.15$; Fe, -0.21; Te, -0.36 (14) vs Dy, $+0.18$; Fe, -0.35; Te, -0.38), which suggests that the Dy–Fe interactions are also more polar, consistent with general expectations. The electron-richer Zr_6MTe_2 phases also exist over pretty much the same range of M. Thus the electron-poorer rare-earth elements do not appear to require an electron-richer M for stability. Rather the zirconium–iron phase fills additional Zr–Fe bonding states, so that the result is still optimized (the COOP is ~ 0 at E_F), while the broad host band is filled somewhat higher.

4. CONCLUSIONS

The compounds Dy_6MTe_2 (M = Fe, Co, Ni) have been prepared through a high-temperature route via arc-melting followed by annealing the compounds for two weeks at 800°C. These compounds adopt Zr_6CoAl_2-type structure, a ternary derivative of the Fe_2P-type structure. The description of the structure in term of the Dy–Dy interactions reflects only part of the stability of the compound; the interstitial Fe and the Te anion in fact both play major roles. The strongest metal–metal bonding occurs within the 1D chains along $\vec{c}$.

ACKNOWLEDGMENTS

The authors are indebted to D.-K. Seo and Paul Maggard for help in the band structure calculations. This research was supported by the National Science Foundation, Solid State Chemistry, via Grants DMR-9510278 and DMR-9809850 and was carried out in the facilities of the Ames Laboratory, DOE.

REFERENCES

1. L. Brewer and P. R. Wengert, *Met. Trans.* **4,** 83 (1973).
2. B. Harbrecht and H. F. Franzen, *J. Less-Common Met.* **113,** 349 (1985).
3. B. Harbrecht, *J. Less-Common Met.* **124,** 125 (1986).
4. B. Harbrecht, *J. Less-Common Met.* **141,** 59 (1988).
5. M. Conrad and B. Harbrecht, *J. Alloys Compd.* **197,** 57 (1993).
6. B. Harbrecht, *Z. Kristallog.* **182,** 118 (1988).
7. R. L. Abdon and T. Hughbanks, *J. Am. Chem. Soc.* **117,** 10,035 (1995).
8. C. Wang and T. Hughbanks, *Inorg. Chem.* **35,** 6987 (1996).
9. R. L. Abdon and T. Hughbanks, *Chem. Mater.* **6,** 424 (1994).
10. M. E. Badding and F. J. DiSalvo, *Inorg. Chem.* **29,** 3952 (1990).
11. J. Neuhausen, E. W. Finckh, W. Ernst, and W. Tremel, *Chem. Ber.* **128,** 569 (1995).
12. P. M. Maggard and J. D. Corbett, *Inorg. Chem.* **38,** 1945 (1999).
13. P. M. Maggard and J. D. Corbett, in preparation.
14. P. M. Maggard and J. D. Corbett, *Inorg. Chem.* **39,** (2000), in press.
15. J. D. Corbett, *J. Alloys Compd.* **229,** 10 (1995).
16. Y.-U. Kwon, S. Sevov, and J. D. Corbett, *Chem. Mat.* **2,** 550 (1990).
17. Y.-U. Kwon and J. D. Corbett, *Chem. Mater.* **4,** 1349 (1992).
18. Sheldrick, M. SHELXS-86. Universität Göttingen, Germany 1986.
19. TEXSAN, Version 6.0, Molecular Structure Corp., The Woodlands, Texas, 1990.
20. (a) R. J. Hoffman, *J. Chem. Phys.* **39,** 1397 (l963); (b) M. Whangbo and R. J. Hoffman, *J. Am. Chem. Soc.* **100,** 6093 (1978).
21. CAESAR. J. Ren, W. Liang, M.-H. Whangbo, North Carolina State University, 1998.
22. L. Pauling, "The Nature of the Chemical Bond," 2nd ed. Cornell Univ. Press, Ithaca, NY, 1960.
23. R. D. Shannon, *Acta Crystallogr. Sect. A* **32,** 751 (1976).
24. A. Kaprzyk, W. Zarek, A. Slebarski, *J. Less-Common Met.* **105,** 231 (1985).
25. P. Villars and L. D. Calvert, "Pearson's Handbook of Crystallographic Data for Intermetallic Phases," 3rd ed., Vol. 1. American Society for Metals, Materials Park, OH, 1985.
26. P. I. Kryiyakevich, V. V. Burnashova, and V. Y. Markiv, *Dopov. Akad. Nauk. Ukr. RSR, Ser. A: Fiz-Tekhn. Mat. Nauki* **32,** 828 (1970).
27. T. Hughbanks, G. Rosenthal, and J. D. Corbett, *J. Am. Chem. Soc.* **110,** 1511 (1988).
28. M. Ebihara, J. D. Martin, and J. D. Corbett, *Inorg. Chem.* **33,** 2079 (1994).
29. A. M. Guloy and J. D. Corbett, to be submitted.
30. A. Alvarez, Tables of Parameters for Extended Hückel Calculations, Parts 1 and 2, Barcelona, Spain, 1987.
31. S.-T. Hong, J. D. Martin, and J. D. Corbett, *Inorg. Chem.* **37,** 3385 (1998).